ACS OMEGA

http://pubs.acs.org/journal/acsodf

Article

Research on the Influence of Combustion Methods on NO_x Emissions from Co-combustion of Various Tannery Wastes

Jiehan Zhang, Hang Yang, Guangyi Zhang,* Guojun Kang,* Zhouen Liu, Jian Yu, and Shiqiu Gao

Cite This: *ACS Omega* 2022, 7, 4110−4120

Read Online

ACCESS | Metrics & More | Article Recommendations

ABSTRACT: To further increase combustion efficiency and reduce nitrogen oxide pollution caused by tannery wastes, three raw materials, including tannery sludge, chrome-tanned buffing dust, and chrome shavings, were burned together in a dual-bed model reactor under various conditions. In addition, a thermogravimetric analysis of co-combustion of three tannery wastes was studied in this study, which was conducive to understanding the combustion characteristics and positive effects. The comprehensive combustibility index S, the flammability index K_r, and the stable combustion characteristic index G_b all increased when the tannery sludge was blended with chrome-tanned buffing dust and chrome shavings, indicating that the combustion behavior was improved by co-combustion. For normal combustion, decreasing the gas volume flow and temperature resulted in a decrease in the oxidation of nitrogen compounds, consequently lowering the NO_x emission. During air staged combustion, at an appropriate secondary gas ratio of about 10−40%, the NO_x reduction would be increased from 10.9 to 19.3%. By increasing the tertiary gas volume flow from 0.2 to 1.1 L/min in decoupling combustion, an average relative NO_x reduction efficiency of 47% was attained compared with normal combustion. The results offered a viable technology that resulted in a lower NO_x emission and realized the application of decoupling combustion.

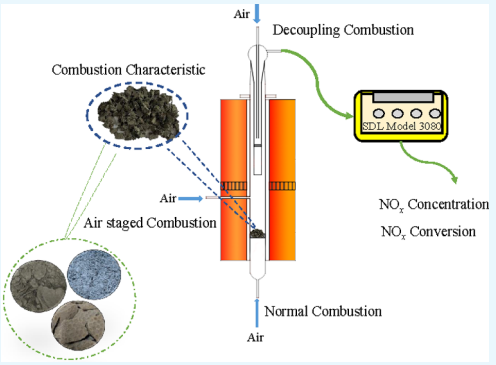

1. INTRODUCTION

China, as the largest producer and exporter of tannery, is suffering from severe tannery wastes pollution caused by improper disposal. Leather scraps and tannery sludge (TS) are all hazardous solid wastes, which can easily cause severe environmental contamination.[1−6] Tannery sludge produced from the tanning industry includes proteins, hair, lime, salts, acids, tannins, dyes, and oils.[7,8] Both chrome-tanned buffing dust (CTBD) and chrome shavings (CS) belong to animal fur and are mainly composed of protein, fat, and inorganic salts. The typical treatment methods for tannery sludge include landfill and composting, but these methods are disadvantageous in terms of land-consumption and long treatment cycles. When leather scraps are used to produce collagen fibers and industrial gelatin, both chromium removal and supervision are complicated. With the advantages of disinfection and sterilization, reduced volume, and flue gas recycling,[9] combustion has significant potential to meet cleaning treatment and energy utilization for tannery wastes. However, considering the low calorific value and high ash content of tannery sludge and its unstable and insufficient combustion process, it is not suitable for burning alone. The co-combustion of biomass and tannery sludge can effectively improve combustion efficiency.[10−12] Through the co-combustion study of sludge and rice husk, Wang et al.[13] found that the combustion points of the mixture decreased after adding rice husk, and the combustion effect was the best when the rice husk dosage was 30%. Since chrome-tanned buffing dust and chrome shavings exhibit the characteristics of low ash and high calorific value, the co-combustion with tannery sludge is feasible.

With high nitrogen content in the tannery wastes, nitrogen oxides (mainly NO) are the major contributors to air pollution during combustion. In addition to the impact on the formation of acid rain, NO_x is also responsible for the formation of photochemical smog. Performances of NO_x emission under different combustion parameters were studied, which serve as a guideline for low NO_x combustion of tannery wastes.[14,15] Zhang et al.[16] investigated the contribution of increased gas volume flow toward NO_x emissions during the normal combustion of sludge, while Zhang et al.[10] observed NO_x reduction during air staged combustion under an increasing secondary gas ratio. Moreover, Zawadzki et al.[17] investigated the interactions of NO_x with carbon by Fourier transform

Received: October 9, 2021
Accepted: January 17, 2022
Published: January 28, 2022

https://doi.org/10.1021/acsomega.1c05640
ACS Omega 2022, 7, 4110−4120

Table 1. Proximate and Ultimate Analyses of Tannery Wastes

	proximate analysis (wt %, d)			ultimate analysis (wt %, daf)					
samples	ash	volatile	fixed carbon	C	H	N	S	O[a]	calorific value/(MJ/kg)
TS	46.75	51.63	1.62	39.60	4.40	2.74	8.38	44.88	8.49
CTBD	9.17	74.75	16.08	57.42	14.25	4.75	2.95	20.63	15.46
CS	14.37	56.95	28.68	65.30	14.51	6.63	2.89	10.67	16.06
TBC	28.35	54.08	17.57	44.55	9.73	4.89	5.89	34.94	13.16

[a]The O content was calculated by subtraction; d: dry basis, daf: dry and ash-free basis.

Table 2. Composition of Ashes of the Three Samples[a]

	composition (wt %)										
samples	CaO	Fe_2O_3	SO_3	Cr_2O_3	Al_2O_3	TiO_2	SiO_2	MgO	P_2O_5	Na_2O	others
TS	42.29	18.99	17.23	4.68	4.12	4.12	3.96	1.75	1.08	1.06	0.72
CTBD	0.89	0.92	10.09	52.89	3.73	0.63	22.81	0.29	3.47	3.99	0.29
CS	0.68	1.06	10.77	78.63	0.27	0.18	0.95	0.71	2.33	4.28	0.14

[a]XRF analysis.

infrared spectroscopy (FTIR), which revealed that char reduction technology could result in decreased NO_x emission. The NO_x emission of decoupling combustion was further decreased by integrating material pyrolysis with char reduction. Relevant studies were carried out regarding the NO_x reduction capacity of the coal decoupling combustion by He et al.[18] Dong et al.[15] found that the rice husk char had a great impact on NO_x reduction that would affect NO_x emission. It was found that the NO_x conversion was lower by 36% than that of normal combustion.

However, there are few fundamental reports on how the NO_x emission varies with the combustion methods for tannery wastes, with limited relevant information obtained. In the present study, the investigation of the combustion characteristics and interaction of tannery wastes was assessed by thermogravimetry−derivative thermogravimetric (TG−DTG) analysis. Also, this study is devoted to achieving low emissions by changing combustion methods. The effect of combustion parameters, including temperature, total volume flow, secondary gas ratio, and tertiary gas volume flow, on NO_x concentration and conversion in the flue gas were analyzed in detail. The aim of the study was to achieve the effective combustion and low NO_x emission of flue gas produced through various tannery wastes.

2. MATERIALS AND METHODS

2.1. Material Characterization. The feedstock for tannery sludge (TS), chrome-tanned buffing dust (CTBD), and chrome shavings (CS) was obtained from a leather products company in Guangdong province, China. After the raw materials were dried, they were crushed and sieved to obtain particles with a diameter of 0.178 mm. Then, the TS, CTBD, and CS were mixed at a weight ratio of 5:2:3 and tableted and crushed to obtain particles with a diameter of 1.6−2.5 mm, denoted TBC. In addition, the pyrolysis char of TS, CTBD, CS, and TBC was prepared at 950 °C under a N_2 atmosphere, which was then used for decoupling combustion. The proximate and ultimate analyses of raw materials are listed in Table 1, which were determined according to the proximate analysis of solid biofuels (GB/T 28731-2012) and ultimate analysis of coal (GB/T 31391-2015) recorded by National Standards of the People's Republic of China, respectively. The calorific value of the samples was measured with an oxygen bomb calorimeter, which was measured by determining the calorific value for solid biofuels (GB/T 30727-2014), as shown in Table 1. As exhibited in Table 2, the main components and species of metal element for TS, CTBD, and CS were tested by determining the ash composition in solid biofuels (GB/T 30725-2014). The results showed that Fe and Ca were plentiful in TS, and more than 55% Cr was present in CTBD and CS.

2.2. Experimental Procedure. The Japan Seiko TG/DTA 6300 thermogravimetric analyzer was used in the experiment to determine the combustion characteristics of raw materials. The nonisothermal experiment was carried out in air with a flow rate of 50 mL/min, and all samples with a uniform mass of 10 mg were preheated from 25 to 1000 °C at a heating rate of 10 °C/min.

All experiments were carried out in a dual-bed model reactor shown schematically in Figure 1. The apparatus mainly consisted of a gas supply system, a dual-bed reactor made of quartz and heated using a two-zone electrical oven, and a flue gas analysis system. The gas supply system included high-purity N_2 and O_2 steel cylinders and three rotameters, controlling the primary, secondary, and tertiary gas. The dual-bed reactor was composed of the following two parts: an

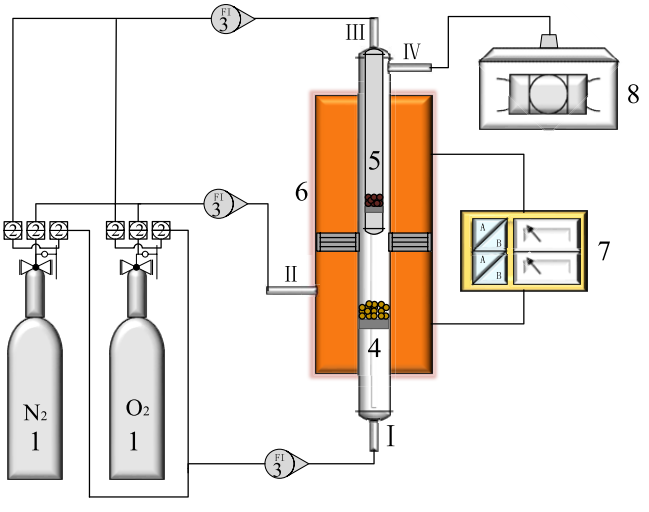

Figure 1. Schematic diagram of the experimental apparatus.

https://doi.org/10.1021/acsomega.1c05640
ACS Omega 2022, 7, 4110−4120

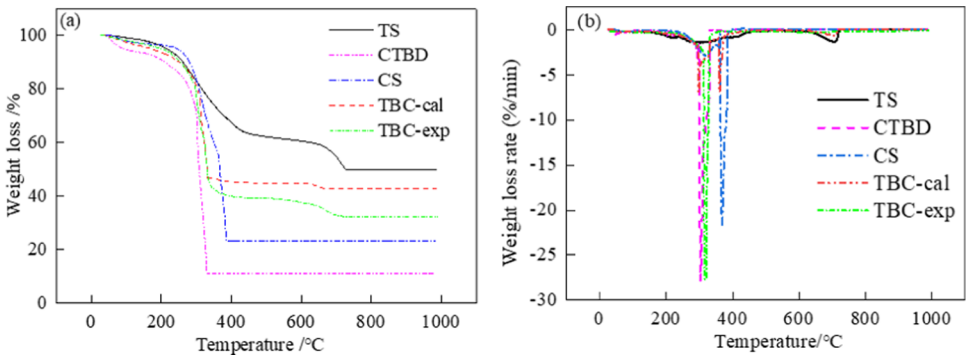

Figure 2. TG curves (a) and DTG curves (b) of samples.

outer tube (30 mm in diameter, 900 mm in height) and an inner tube (25 mm in diameter, 550 mm in height). A 0.425 mm quartz sand sintered plate was arranged on the upper and the lower part of the reaction section to place the pyrolysis char and raw materials. In the flue gas analysis system, an infrared flue gas analyzer (SDL model 3080) monitored the flue gas composition in real time. This experiment defined the initial condition of combustion as a decrease of O_2 content, and when the O_2 content recovered to about 21%, it was deemed that the combustion ended. During the simulated experiment, normal combustion, air staged combustion, and decoupling combustion, to facilitate comparison, the quality of materials and the total concentration of O_2 needed were kept constant. The average value of three parallel measurements was taken as the final result, and the error was controlled within 2%.

In normal combustion, the combustion occurred only in the primary gas. A mixed gas of O_2 and N_2 with an oxygen content of 21% was introduced to position I, and 0.5 g of materials was placed on the lower sieve.

Air staged combustion separated the reaction by controlling the ratio of primary and secondary gas. The primary gas helped the low-oxygen combustion of materials, and the secondary gas promoted the burning of flue gas. NO_x emissions could be reduced by adjusting the ratio of primary and secondary gas.[19] To simulate air staged combustion, 0.5 g of materials was placed on the lower sieve, and O_2 and N_2 mixed gas with 21% oxygen concentration of different volume flows was introduced at positions I and II.

Decoupling combustion had a pyrolysis zone and a combustion zone. The raw materials were pyrolyzed in position I (0.2 L/min N_2). The pyrolysis gas generated in this process was burned in position II (0.8 L/min O_2 and N_2 mixed gas with 26.3% oxygen concentration), and residual volatiles in char and other unburned gaseous components were burned in position III (O_2 and N_2 mixed gas with 21% oxygen concentration). In decoupling combustion, the lower sieve of the reactor was the pyrolysis zone (0.5 g of materials), and the upper part was the combustion zone, which contained the char produced by pyrolysis. The whole reaction was equivalent to the combustion of 0.5 g of materials. Furthermore, the Cr valence state of decoupling combustion ash was studied using an X-ray photoelectron spectroscopy (ESCALAB 250Xi, Thermo Fisher Scientific, America).

2.3. Characterization. *2.3.1. Combustion Characteristic Parameters.* To study the combustion characteristics of TS, CTBD, CS, and TBC, the following indicators were mainly investigated: ignition temperature T_i, peak temperature T_{max}, and burnout temperature T_h. The formulas of the flammability index K_r, stable combustion characteristic index G_b, and a comprehensive combustibility index S could be defined as in eqs 1−3.[20]

$$K_r = \frac{(dw/dt)_{max}}{T_i^2} \quad (1)$$

$$G_b = \frac{(dw/dt)_{max}}{T_{max} T_i} \quad (2)$$

$$S = \frac{(dw/dt)_{max}(dw/dt)_{mean}}{T_i^2 T_h} \quad (3)$$

where $(dw/dt)_{max}$ and $(dw/dt)_{mean}$ represent the maximum and average mass loss rates, respectively. In the formula $(dw/dt)_{mean} = G_{ash}/t_h$, G_{ash} represents the weight loss corresponding to the temperature when the fuel combustion lost 98% of the weight and t_h is the burnout time.

2.3.2. Evaluation of the Conversion of Fuel N to NO. In this experiment, N_2O and NO_2 concentrations in flue gas were normally lower for all combustion processes and therefore could be neglected with regard to nitrogen balance in this study. The conversion fraction of fuel nitrogen to NO (x_N) can be calculated as in eq 4.[18]

$$x_N = \frac{M_{NO}/30}{mW_N/14} \quad (4)$$

where m is the sample weight (g), W_N is the nitrogen mass fraction in the sample (%), and M_{NO} is NO mass in the flue gas, which can be obtained by the numerical integration of the measured NO concentration in flue gas C_{NO} over the whole period from the onset until completion of each process, according to eq 5.

$$M_{NO} = \frac{30}{22.4} \times \int_{t_1}^{t_2} C_{NO} V dt \quad (5)$$

where t_1 and t_2 are the start time and end time (min) of the experiment, respectively, and V is the flue gas flow rate (in L/min, at 1 atm and 0 °C), which can be approximated by the measured total inlet gas flow rate.

3. RESULTS AND DISCUSSION

3.1. Combustion Characteristics. As shown in Figure 2, the mass loss of TS, CTBD, CS, and TBC as a function of temperature was depicted in TG and DTG curves during the combustion process. The combustion process of TS could be divided into two stages, the volatile combustion stage and the

https://doi.org/10.1021/acsomega.1c05640
ACS Omega 2022, 7, 4110−4120

Table 3. Combustion Characteristic Parameters of Different Samples

samples	T_i /°C	T_{max}/°C	T_h/°C	$K_r(10^{-3})/(min/°C^2)$	$G_b(10^2)/(min/°C)$	$S(10^{-6})/(min^{-2}/°C^3)$
TS	224	706	731	2.26	0.46	0.86
CTBD	175	306	337	89.75	15.72	25.02
CS	179	368	392	67.90	10.58	29.93
TBC	175	315	700	92.96	15.81	32.14

coke combustion stage.[21] The dominating combustion stage included the release of volatile matter, occurring between 200 and 450 °C. An obvious peak appeared at 307 °C with an intense reaction occurring.[22] The mass loss of the coke combustion stage (450−700 °C) was determined by the oxidation of the char attributed to the nondegradable macromolecule depolymerization; the weight loss during the entire combustion process was 61.3%. Different from TS, CTBD and CS were polymers with high volatile contents, which have a low decomposition temperature. The mass loss for combustion of CTBD and CS went through two stages, moisture evaporation and both combustion of volatile and char. The main mass loss was the second stage for CTBD and CS, caused by the intensive decomposition of lignin at 200−400 °C. In the whole combustion process, the mass losses of CS and CTBD were related to the properties and structures, accounting for 89.2 and 76.3%, respectively.[13,21] In addition, TS exhibited a higher ignition and burnout temperature, which was ascribed to the calorific value and ash content. The intensive combustion of the three raw materials partially overlapped at 300−400 °C, and so it was speculated that there may be a mutual propelling effect during co-combustion.[23] According to the TG−DTG curves for TBC, the mass loss of TBC was dominated by volatile combustion, and the second peak value of DTG was unapparent. To assess the interaction effect during co-combustion, the calculated TG and DTG curves of TBC were obtained by eq 6

$$TG_{cal} = x_{TS}TG_{TS-exp} + x_{CTBD}TG_{CTBD-exp} + x_{CS}TG_{CS-exp} \quad (6)$$

where x represents the blending ratio of the sample corresponding to the individual fuel in TBC. As shown in Figure 2a, there were obvious differences between experimental and calculated values, which suggested that the synergistic effect existed at 370 °C. In comparison of the calculated value, the experimental DTG curve moved into a low temperature and reached the peak at approximately 314 °C, indicating a positive effect during co-combustion.

Based on the TG−DTG analysis, Table 3 shows the combustion characteristic of different materials. The indices K_r, G_b, and S represent the flammability of samples, combustion rate, and burnout characteristics. Considering the values of indices K_r, G_b and S synthetically, the larger these three values were, the better the combustion performance of the sample was.[20,24] As for TS, the value of the indices less than CTBD and CS was considered as performing a worse combustion characteristic, and so it was not suitable for burning alone. When TBC burned, the intensity of volatiles released was remarkably promoted by each other, and so the combustion characteristic could be prominently improved. As shown in Table 2, the synergistic effect was attributed to the fact that the metal element could act as a catalyst to facilitate the interaction of the material with oxygen, hence leading to improved combustion efficiency.

3.2. Comparison of NO_x Emission Characteristics of Different Materials in the Three Combustion Methods.

Experimental conditions of normal combustion, air staged combustion, and decoupling combustion described in the following paragraphs are summarized in Table 4, which shows the combustion parameters for TS, CTBD, and CS.

Table 4. Experimental Conditions of Various Combustion Processes

combustion process		normal combustion	air staged combustion	decoupling combustion
I	volume flow, L/min	1.5	1.0	0.2
	O_2 concentration, %	21	21	0
II	volume flow, L/min		0.5	0.8
	O_2 concentration, %		21	26.3
III	volume flow, L/min			0.5
	O_2 concentration, %			21
total inlet gas	volume flow, L/min	1.5	1.5	1.5
	O_2 concentration, %	21	21	21

Figure 3 depicts the NO_x concentration and conversion in different raw materials with the variation of combustion methods. As per the ultimate analysis data (Table 1), the examined nitrogen contents of tannery wastes were in the descending order as CS (6.63%) > CTBD (4.75%) > TS (2.74%), consistent with the NO_x emission during the combustion process. So, in view of such comparisons, a visible connection was seen among nitrogen contents of tannery wastes regarding NO_x conversion. Under air staged combustion, there was no significant difference in NO_x reduction for TS, CTBD, and CS compared with normal combustion. But, among these processes, decoupling combustion exhibited the best performance with respect to NO_x emission. The average NO_x conversion of decoupling combustion was generally 30% lower than that of normal combustion, which reduced the NO_x emission by 32.1, 34.1, and 36.3% for TS, CTBD, and CS, respectively. The significant influence of tannery waste type on NO_x reduction could be supported by this study during decoupling combustion, where lower T_i and higher volatiles from CTBD and CS promoted higher NO_x reduction efficiency than those from TS.[25,26] It was concluded that decoupling combustion was friendly to low NO_x emission for high nitrogen content material. It might give better treatment for different materials that were suitable for controlling NO_x emission.

3.3 Influence of Normal Combustion on NO_x Emissions.

The measured concentrations of CO_2, O_2, and NO_x in flue gas for TBC combustion with 1.5 L/min primary

https://doi.org/10.1021/acsomega.1c05640
ACS Omega 2022, 7, 4110−4120

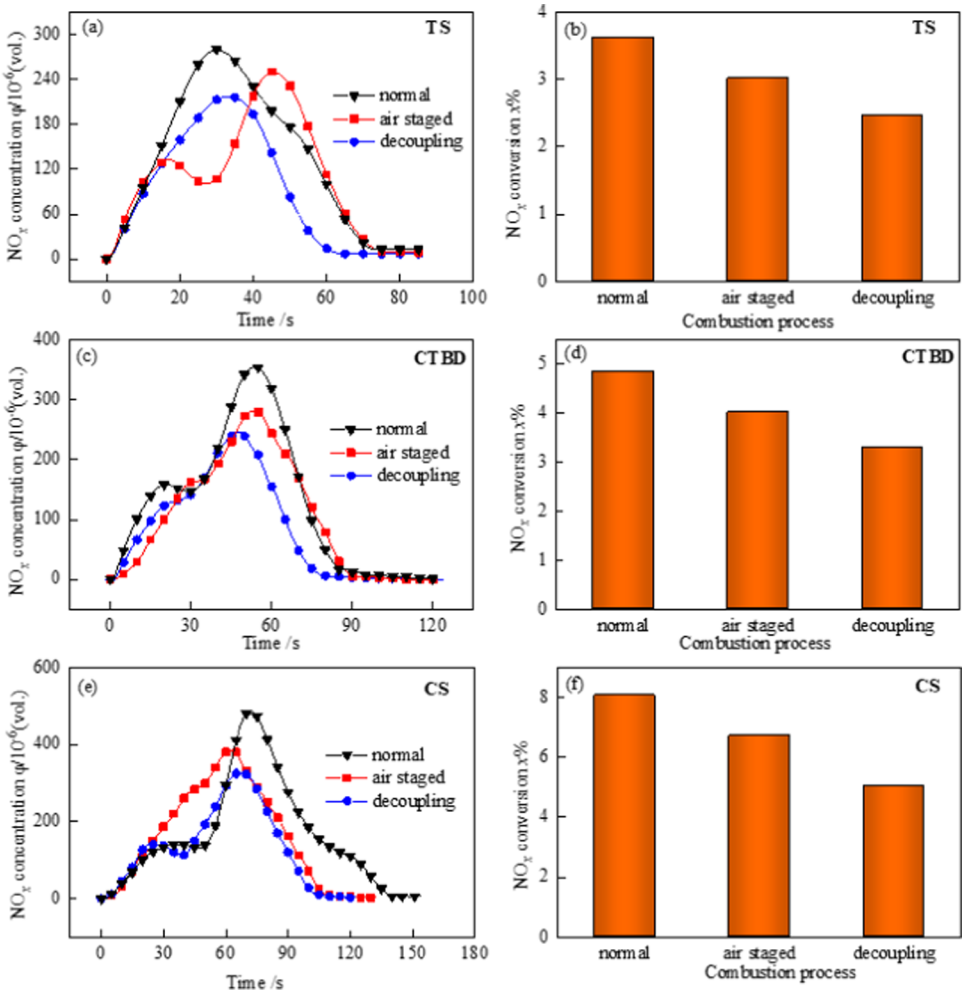

Figure 3. Variations of NO_x concentration ((a) TS, (c) CTBD, and (e) CS) and fuel nitrogen conversion to NO_x ((b) TS, (d) CTBD, (f) CS) for different materials in different combustion processes.

gas and 850 °C are plotted in Figure 4. At the TBC combustion initial stage, its oxidation rate increased, resulting in a sharp increase in CO_2 and NO_x concentrations with different degrees and a decrease in O_2 concentration. With a longer combustion time, the CO_2 concentration reached a maximum value of 12%, and in the meantime, the NO_x concentration decreased sustainably, which maintained its minimum values and then reached a maximum value of 385 ppm. It was considered that the N in TBC formed by pyridine and pyrrole with high thermal stability could be released at a higher temperature.[18] According to the O_2 content change curve, combustion occurred under sufficient oxygen conditions where the N was fully converted. The results obtained through the work provided valuable information regarding NO_x emission under different combustion methods. Therefore, the next work was focused on NO_x reduction by varying the combustion parameters to achieve optimum NO_x reduction efficiencies.

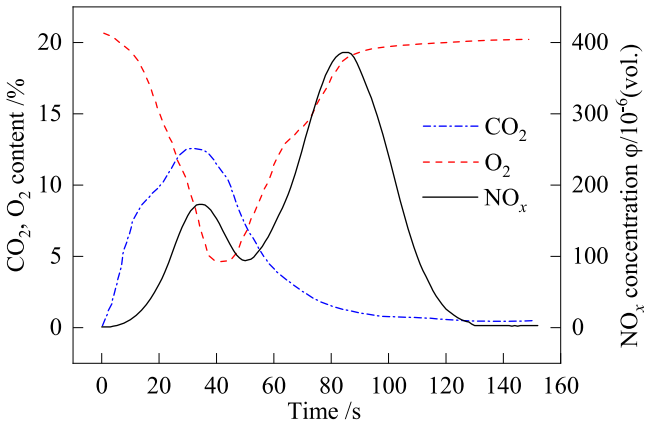

Figure 4. Profiles of CO_2, O_2, and NO_x in flue gas during WML combustion.

3.3.1. NO_x Emission Varying with Volume Flow. Figure 5 describes the NO_x concentration and conversion in the TBC sample under different volume flows at 850 °C, and the only variable was the primary gas volume flow, which was 1.2, 1.5, 1.8, and 2.1 L/min. Tannery wastes were a chain compound formed by the combination of N and C−H compounds. The bond energy of C−N was less than that of N−N, and so C−N easily broke during the combustion. NO was formed through fractured nitrogen reacting with hydrocarbon radicals in fuel-rich regions of flames consequently oxidized to form NO.

In addition, fuel intrinsic nitrogen could either evolve during the devolatilization stage of combustion (referred to as volatile-N) or retain in the char (referred to as char-N).[27] The two peaks, as shown in Figure 5a, just correspond to the burning of

https://doi.org/10.1021/acsomega.1c05640
ACS Omega 2022, 7, 4110−4120

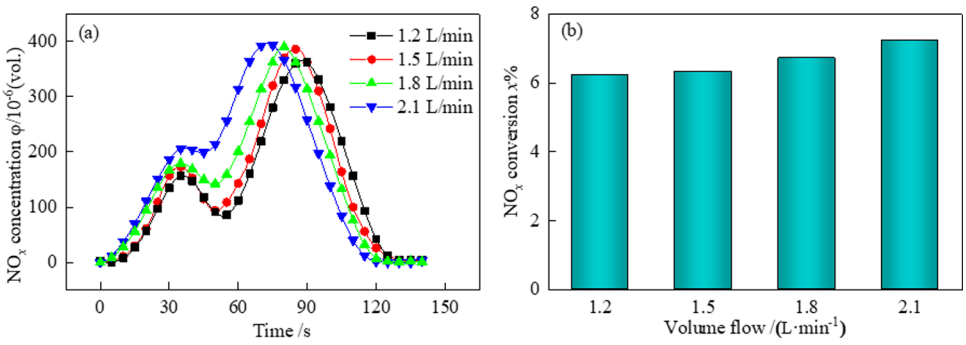

Figure 5. Variations of NO_x emission (a) and NO_x conversion (b) with different volume flow rates.

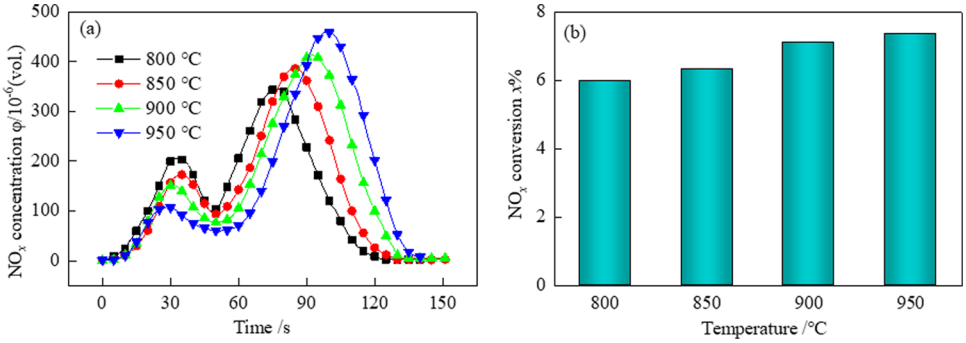

Figure 6. Variations of NO_x emission (a) and NO_x conversion (b) at different combustion temperatures.

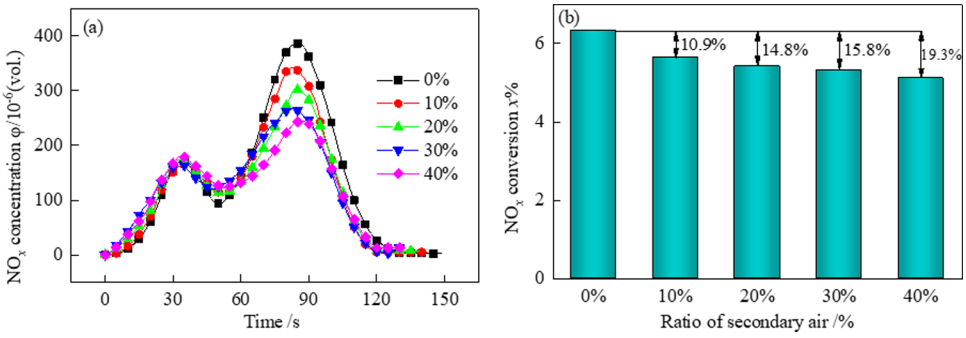

Figure 7. Variation of NO_x emission (a) and NO_x conversion (b) with different ratios of secondary air.

both volatile-N and char-N.[28] Due to the rapid precipitation of volatile nitrogen, it could be reduced by reductive gas, and the peak partially overlapped with char nitrogen. In the case of TBC, a significant amount of CH_4 and H_2 might be released directly during the devolatilization phase to be reduced to N_2 through the following reactions[29,30]

$$CH_4 + 2NO_2 \rightarrow CO_2 + N_2 + 2H_2O$$

$$2NO + 2H_2 \rightarrow N_2 + 2H_2O$$

Because of these reactions in the combustion process, the NO_x emission was higher during the later combustion period to indicate the contribution of char nitrogen species. And the release and combustion of fuel would share more instantaneous variations and reaction complexity, which depended upon temperature, residence time, and volume flow. Figure 5 shows that the measured NO_x emission was higher for the higher volume flow; it was predictable that when the volume flow increased from 1.2 to 2.1 L/min, the volatile and char were more likely to be oxidized and accelerate the NO_x conversion from 6.2 to 7.2%.[14] The increase of volume flow would also vary the disturbance effect in flue gas to indicate the potential influence of residence time in the reactor, and it rendered the peak time earlier for the NO_x emission.

The increase in rate was more significant when the volume flow exceeded 1.5 L/min. Hence, while ensuring the complete combustion of the raw materials, appropriately reducing the volume flow will help the low-NO_x emission.

3.3.2. NO_x Emission Varying with Temperature. Based on the experiment above, Figure 6 presents the change trends of NO_x concentration and its corresponding NO_x conversion by varying the incineration temperature at 1.5 L/min volume flow. As for the NO_x concentration (Figure 6a), the peak of volatile nitrogen experienced a gradual decrease, and the peak of coke nitrogen amplified as the temperature increased. The corresponding conversion of fuel-N to NO_x (Figure 6b) also increased from 5.9 to 7.4%. As the incineration temperature increased, a part of char would be promoted due to the acceleration of gas diffusion, which resulted in a gradual sufficiency of the combustion process. This phenomenon could be attributed to the fact that the increase in NO_x concentration was related to the intensified release of HCN and NH_3,

https://doi.org/10.1021/acsomega.1c05640
ACS Omega 2022, 7, 4110−4120

occurring in the reactions including HCN + O → NCO + H and HCO + O → NO + CO.[18] When the combustion temperature was above 850 °C, the release of volatile matters from TBC became faster enough, but the gas residence time inside the reactor became shorter. This would weaken the reduction to the released nitrogen intermediates and formed NO_x.[31] It is worth mentioning that the peak time of the maximal peak NO_x formation appeared at a relatively longer time with the increasing temperature.

According to Figure 6b, with the increase of the incineration temperature from 800 to 850 °C, the NO_x conversion increased by 0.36%, and then it tended to a substantial increase of about 0.78% from 850 to 900 °C. Therefore, it could be concluded that 800−850 °C was conducive to low NO_x emission of TBC.

3.4. Influence of Secondary Gas on NO_x Emissions during Air Staged Combustion. Figure 7 shows air staged combustion results of NO_x concentration and conversion at 850 °C and 1.5 L/min for TBC. When the total volume flow was 1.5 L/min, the NO_x concentration and NO_x conversion gradually decreased on increasing the second gas ratio from 10 to 40%. Figure 7 demonstrates essentially that an increase in the secondary gas decreased the NO_x emission at a specific high reduction atmosphere in the primary combustion zone due to the increased combustion atmosphere reduction capability from increasing the reductive gas content such as CO, CH_4, etc.[29] The higher CH_4 and CO contents and lower O_2 concentration formed at the primary combustion zone inhibited the process of intermediates such as HCN and NH_3 converting to NO_x.[3030] In addition, the reduction time of char-N had to extend as well with increasing secondary gas because of the retrorse gas atmosphere and also too long flue gas residence time inside the reactor.[32] As seen in Figure 7b, the NO_x conversion decreased from 6.3 to 4.9% at the secondary gas ratio range from 10 to 40%, and the NO_x reduction rate increased from 10.9 to 19.3% compared with normal combustion, indicating that the air staged combustion was theoretically feasible for the reduction of NO_x emission. Nonetheless, the decrease of NO_x conversion with increasing second gas appeared gradually slower when the second gas ratio was 20%. It was possibly because the reduction in the primary gas was already enough, rendering the further decrease of the NO_x conversion more difficult.

3.5. Influence of Tertiary Gas on NO_x Emissions during Decoupling Combustion. Pyrolysis is the first stage of decoupling combustion, and both pyrolysis gas and char produced from pyrolysis affect the reduction process of decoupled combustion. According to our previous research,[19] the pyrolysis gas was mainly composed of H_2, CH_4, CO, CO_2, and C2−C3, and the concentrations were 47.0, 9.8, 19.5, 15.6, and 2.8 mL/g, respectively; the content of reducing gas was relatively low. NO_x reduction by char was the major contribution with decoupling combustion, and the NO_x reduction fraction could reach about 90% according to the experimental results described by Cai et al.[29] Thus, the NO_x reduction mechanism of decoupling combustion mainly started from the effect in char according to Tomita.[33] The NO_x reduction by char was a complex process, involving the initial chemisorption of NO and the reactions on the char surface. The possible routes for NO reduction by char could be as follows

$$NO + 2C^* \rightarrow C(N) + C(O)$$

$$C(N) + NO \rightarrow N_2 + C(O)$$

$$2C(N) \rightarrow N_2 + 2C^*$$

where C*, C(N), and C(O) denote the surface free site, surface nitrogen, and oxygen species, respectively. In addition, during the decoupling combustion process, pyrolysis gas such as CO, H_2, and CH_4 might be produced. With the reductive effect of char, NO_x could also be reduced by CO, H_2, and CH_4 as described in the reactions.[34,35]

$$CO + NO \rightarrow CO_2 + N_2$$

$$H_2 + NO \rightarrow H_2O + N_2$$

$$CH_4 + NO_2 \rightarrow CO_2 + N_2 + H_2O$$

On the other hand, HCN was considered the dominant product during the decoupling combustion for CTBD and CS.[36] It was estimated that the NO_x reduction was undertaken from HCN, which, once formed, followed the reaction pathway as HCN + O → NCO + H → H_2 + N.[37] Thus, analysis of the reduction from the char was further performed in the next section to understand the decoupling combustion.

The reaction gas mixture consisting of 200 ppm NO, 5 vol % O_2, and N_2 balance was fed into the reaction system through mass flow controllers with a total flow rate of 500 mL/min at a gas hourly space velocity of 9200 h^{-1}, calculating the reduction rate of char to NO, and the results are shown in Figure 8.

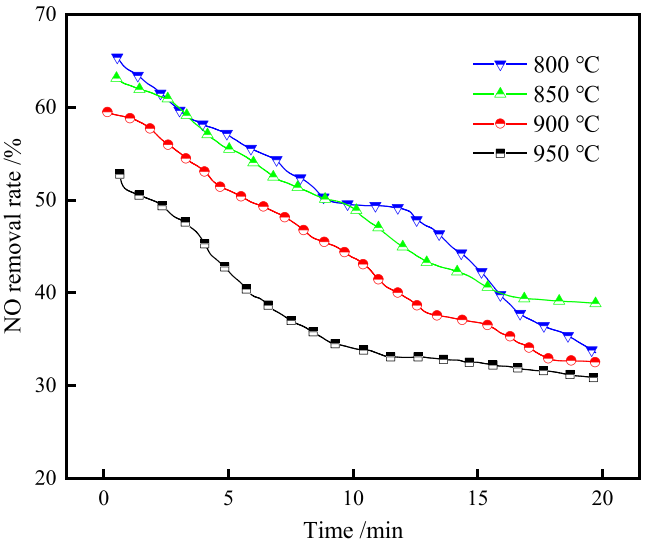

Figure 8. Effect of reaction temperature on the NO removal rate.

Figure 8 depicts the trend of the NO reduction by char for increasing the reaction time at different furnace temperatures. The NO removal rate by char was decreased by increasing the furnace temperature from 800 to 950 °C as further increases in temperature enhanced the combustion of char, which consequently resulted in the conversion of nitrogen materials into NO. In addition, the chemical adsorption active sites on the char surface were slowly consumed,[38] and so the initial NO removal rate decreased from 65 to 52%. For a NO removal curve at the same temperature, with the increasing reaction time, the reducing layer of char was constantly consumed, and the reduction effect of NO was reduced. The higher reduction of NO on the char surface under 850 °C when the response time exceeded 15 min was because the C(O) formed by

https://doi.org/10.1021/acsomega.1c05640
ACS Omega 2022, 7, 4110−4120

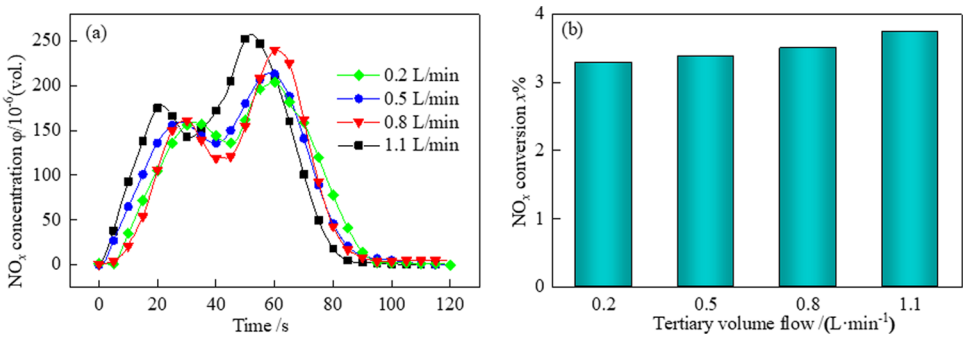

Figure 9. Variations of NO_x emission (a) and NO_x conversion (b) with different tertiary volume flows.

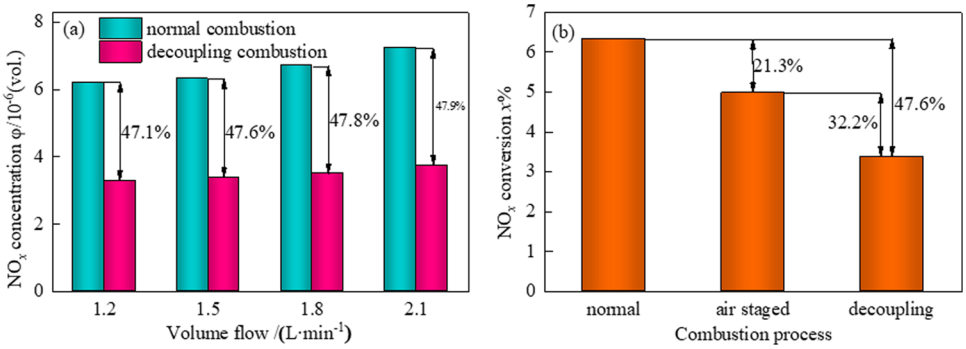

Figure 10. NO_x conversion in normal or decoupling combustion with different volume flows (a) and NO_x emission reduction rates of different combustion modes (b).

Table 5. Composition of Ashes of Decoupling Combustion[a]

	composition (wt %)										
samples	CaO	Fe_2O_3	SO_3	Cr_2O_3	Al_2O_3	TiO_2	SiO_2	MgO	P_2O_5	Na_2O	others
ash	23.92	10.96	17.42	27.32	3.51	2.01	8.25	1.02	1.31	2.35	1.93

[a]XRF analysis.

chemical adsorption directly reacted with NO and decomposed to C*, which had high affinity to engulf NO, thus re-engaging in the reduction reaction of NO.[39] Therefore, the temperature of 850 °C was favorable to reduce NO, which was better for the decoupling combustion of various tannery wastes.

Figure 9 shows the NO_x concentration and its corresponding NO_x conversion at 850 °C but a different volume flow of tertiary gas in the combustion agent. By comparing the NO_x emission trends in Figure 9a, a prominent difference in the NO_x concentration was observed under various tertiary gas volume flows. The NO_x concentration approached its peak level in a longer time when the tertiary gas volume flow increased from 0.2 to 0.8 L/min due to the increase of flue gas being obstructed.[16] It took more time for the reduction of NO_x with the char layer until the great mass of NO_x was converted into N_2.[3535] Based on Figure 9b, the increase of NO_x conversion was exaggerated inversely with increasing tertiary gas volume flow. On the one hand, the increase of air volume flow promoted the oxidation reaction; on the other hand, the increase of tertiary gas volume flow promoted the reduction of char. Thus, the NO_x conversion gradually increased until the tertiary gas volume flow was 1.1 L/min, and the average increase in NO_x conversion was recorded to be 4.39% for an increase in the tertiary gas volume flow from 0.2 to 1.1 L/min. Therefore, an insignificant increase was observed in the NO_x conversion rate, and properly controlling the tertiary gas was conducive to the low NO_x co-combustion of tannery wastes.

Figure 10a shows a comparison of the NO_x conversion between normal combustion and decoupling combustion at the same total volume flow. By further pursuing the calculations, average 47% NO_x reduction efficiency was achieved when the total volume flow was allowed to increase from 1.2 to 2.1 L/min. This clarified that the dominant factor determining the NO_x emission was the reduction of char, an obviously reasonable result on fuel combustion.

Figure 10b shows the NO_x conversion obtained from various combustion processes. In normal combustion and air staged combustion processes, a part of volatile matters might burn within the char layer, reducing the possibility of NO_x being reduced by char. However, the NO_x would pass through the burning char layer, where a considerable part of NO_x could be reduced in decoupling combustion. The NO_x conversion of decoupling combustion was 47.6 and 32.2% lower than that of normal and air staged combustion, respectively. Moreover, by keeping the same conditions of 850 °C and 1.5 L/min, the NO_x reduction rate compared with normal combustion was calculated to be 32.1, 34.1, and 36.3% obtained by TS, CTBD, and CS, respectively. The NO_x reduction rate of TBC reached 47.6%, which was recorded to be much higher than that of single raw materials. Therefore, it was evident that the decoupling co-combustion of various tannery wastes exhibited

https://doi.org/10.1021/acsomega.1c05640
ACS Omega 2022, 7, 4110−4120

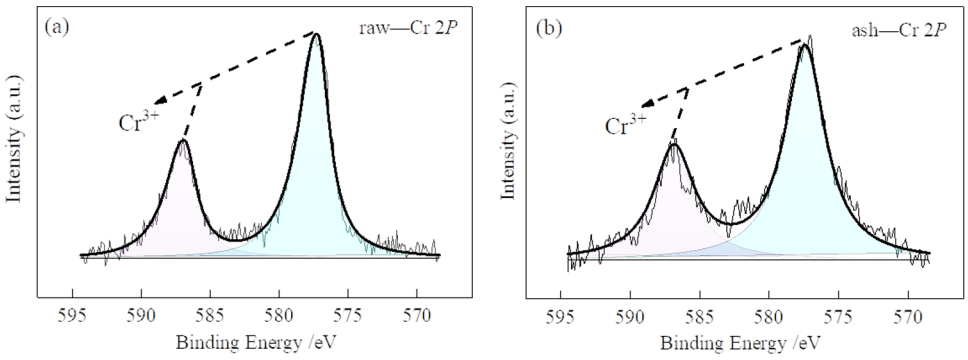

Figure 11. Spectra of XPS for Cr 2p of material (a) and ash (b).

the best performance with respect to NO_x emission and also promoted the combustion process.

3.6. Analysis of Residue Composition after Decoupling Combustion. The NO_x emission was measured during decoupling combustion; in addition, this experiment also analyzed the composition of combustion ash, as shown in Table 5. After decoupling combustion, the main composition of ash did not change obviously, but the content of ash changed. In all of the components of ash, chromium compounds occupied the highest content. Chromium generally included two valence states, Cr(III) and Cr(VI), of which Cr(VI) was more toxic and harmful to the human environment.[40] Thus, this part investigated the valence state of chromium in the ash composition before and after decoupling combustion, which can determine the difficulty and feasibility of its subsequent treatment.

As seen in Figure 11, the valence state of Cr remained trivalent before and after decoupling combustion. When the combustion temperature exceeded 600 °C, Cr(III) was easily oxidized to Cr(VI) during the combustion process, which could lead to severe difficulties in ash disposal.[6] According to the results of this experiment, the reducing environment provided by decoupling combustion effectively inhibited the conversion of Cr(III) to higher valence states, and thus, the ash toxicity was reduced. Moreover, the ash containing Cr(III) could be effectively removed by acidic or alkaline solutions, and the leachate could be used in the chromium tanning process or the electroplating industry.[41] The ash treated with dechromium could basically satisfy the landfill standard for solid wastes containing chromium, in which decoupling combustion played an important role.

4. CONCLUSIONS

The combustion processes of tannery wastes were studied experimentally in a dual-bed reactor. The main objective of the study was to contribute toward achieving the clean combustion of tannery wastes by controlling the emission of NO_x in flue gas. In this study, an experimental investigation of NO_x emission of tannery wastes combustion through various combustion methods was researched. The following conclusions could be drawn:

(1) For the co-combustion of tannery wastes by thermogravimetric analysis, the combustion parameters such as the comprehensive combustibility index S, stable combustion characteristic index G_b, and the flammability index K_r were enhanced, which indicated the combustion processes, whereas effective combustion could be achieved through the co-combustion of tannery wastes.

(2) By changing the combustion methods for TS, CTBD, and CS, decoupling combustion was better for reducing the NO_x emission of raw materials with high nitrogen content. For air staged combustion, there was little effect on the NO_x emissions of materials with various nitrogen content.

(3) At a sufficiently high gas volume flow and reaction temperature, the nitrogen substance in TBC would be oxidized to cause a higher NO_x emission during normal combustion. Under air staged combustion, the increased secondary gas ratio led to a much lower NO_x emission. When the tertiary gas volume flow increased, the NO_x emission increased slightly; however, the average NO_x reduction was about 47% compared with normal combustion at the same volume flow.

(4) Because of the impact of decoupling combustion on NO_x reduction, the NO_x conversion was lower by 47.6% than that of normal combustion under the same conditions. Compared with air staged combustion, the 32.2% NO_x reduction was observed in the decoupling combustion. Moreover, decoupling combustion could effectively inhibit the conversion of chromium in materials to a higher state at a high temperature, which was beneficial to the harmless treatment of ash. Overall, the present work was applicable to tannery wastes by decoupling combustion to achieve cleaner treatment with low NO_x emissions and provided the possibility of integrated treatment of tannery wastes.

AUTHOR INFORMATION

Corresponding Authors

Guangyi Zhang − *School of Ecology and Environment, Beijing Technology and Business University, Beijing 100048, China;* orcid.org/0000-0003-0994-211X; Email: gyzhang@btbu.edu.cn

Guojun Kang − *Institute of Low Carbon Energy, China University of Mining and Technology, Xuzhou 221000, China*; Email: gjkang@cumt.edu.cn

Authors

Jiehan Zhang − *Institute of Low Carbon Energy, China University of Mining and Technology, Xuzhou 221000, China; State Key Laboratory of Multiphase Complex Systems, Institute of Process Engineering, Chinese Academy of Sciences, Beijing 100190, China*

Hang Yang − *State Key Laboratory of Multiphase Complex Systems, Institute of Process Engineering, Chinese Academy of Sciences, Beijing 100190, China*

https://doi.org/10.1021/acsomega.1c05640
ACS Omega 2022, 7, 4110−4120

Zhouen Liu − *State Key Laboratory of Multiphase Complex Systems, Institute of Process Engineering, Chinese Academy of Sciences, Beijing 100190, China*

Jian Yu − *State Key Laboratory of Multiphase Complex Systems, Institute of Process Engineering, Chinese Academy of Sciences, Beijing 100190, China;* orcid.org/0000-0003-0392-2556

Shiqiu Gao − *State Key Laboratory of Multiphase Complex Systems, Institute of Process Engineering, Chinese Academy of Sciences, Beijing 100190, China;* orcid.org/0000-0003-3421-5416

Complete contact information is available at: https://pubs.acs.org/10.1021/acsomega.1c05640

Notes

The authors declare no competing financial interest.

■ ACKNOWLEDGMENTS

This work was financially supported by the Fundamental Research Funds for the Central Universities (2017XKQY065).

■ REFERENCES

(1) Ge, S.; Wang, Q.; Diao, S.; Wang, X.; Yuan, Y.; Luan, J. Research progress and application of solid leather waste. *Leather Chem.* **2019**, *36*, 37−42.

(2) Tan, Q.; Liao, D.; Wan, Y.; Zhu, H. Research on comprehensive utilization technology and new progress of solid waste in leather making. *Leather Manuf. Environ. Technol.* **2020**, *1*, 37−39.

(3) Velusamy, M.; Chakali, B.; Ganesan, S.; Tinwala, F.; Venkatachalam, S. S. Investigation on pyrolysis and incineration of chrome-tanned solid waste from tanneries for effective treatment and disposal: an experimental study. *Environ. Sci. Pollut. Res.* **2020**, *27*, 29778−29790.

(4) Shah, I. A.; Gou, X.; Zhang, Q.; Wu, J.; Wang, E.; Liu, Y. Experimental study on NO_x emission characteristics of oxy-biomass combustion. *J. Cleaner Prod.* **2018**, *199*, 400−410.

(5) Li, Y.; Guo, R.; Lu, W.; Zhu, D. Research progress on resource utilization of leather solid waste. *J. Leather Sci. Eng.* **2019**, *1*, 1−17.

(6) Zhou, Y.; Chen, Z.; Gong, H.; Yang, Z. Chromium speciation in tannery sludge residues after different thermal decomposition processes. *J. Cleaner Prod.* **2021**, *314*, No. 128071.

(7) Silva, J. D.; Leal, T. T.; Araujo, A. S.; Araujo, R. M.; Gomes, R. L.; Melo, W. J.; Singh, R. P. Effect of different tannery sludge compost amendment rates on growth, biomass accumulation and yield responses of Capsicum plants. *Waste Manage.* **2010**, *30*, 1976−1980.

(8) Alibardi, L.; Cossu, R. Pre-treatment of tannery sludge for sustainable landfilling. *Waste Manage.* **2016**, *52*, 202−211.

(9) Tang, P.; Zhao, Y.; Xia, F. Thermal behaviors and heavy metal vaporization of phosphatized tannery sludge in incineration process. *J. Environ. Sci.* **2008**, *20*, 1146−1152.

(10) Zhang, H.; Lv, C.; Li, J.; Qin, W.; Hu, Y.; Dong, C. Solid waste mixtures combustion in a circulating fluidized bed: Emission properties of NO_x, dioxin, and heavy metals. *Energy Procedia* **2015**, *75*, 987−992.

(11) Dong, H.; Jiang, X.; Lv, G.; Wang, F.; Huang, Q.; Chi, Y.; Yan, J.; Yuan, W.; Chen, X.; Luo, W. Co-combustion of tannery sludge in a commercial circulating fluidized bed boiler. *Energy Fuels* **2017**, *31*, 11069−11077.

(12) Shu, Z.; Xu, L. Experimental study on the mixing of tanning sludge and coal. *Energy Environ.* **2007**, *17*, 17−19.

(13) Wang, C.; Bi, H.; Lin, Q.; Jiang, X.; Meng, K.; et al. Thermal characteristics, kinetics, and volatility of co-combustion of sewage sludge and rice husk. *Bioenergy Res.* **2021**, *14*, 1014−1024.

(14) Zhan, M.; Sun, C.; Chen, T.; Li, X. Emission characteristics for co-combustion of leather wastes, sewage sludge, and coal in a laboratory-scale entrained flow tube furnace. *Environ. Sci. Pollut. Res.* **2019**, *26*, 9707−9716.

(15) Dong, L.; Gao, S.; Xu, G. NO Reduction over biomass char in the combustion process. *Energy Fuels* **2010**, *24*, 446−450.

(16) Zhang, L.; Zhou, G.; Guo, Z.; Zhong, W.; Xu, P. Application and pollutant emission characteristics of sludge co-incineration. *Chem. Eng. Equip.* **2020**, *12*, 7−8.

(17) Zawadzki, J.; Wisniewski, M.; Weber, J.; Heinta, O.; Azambre, B. IR study of adsorption and decomposition of propan-2-ol on carbon and carbon-supported catalysts. *Carbon* **2001**, *39*, 187−192.

(18) He, J.; Song, W.; Gao, S.; Dong, L.; Mirko, B.; Li, J.; Lin, W. Experimental study of the reduction mechanisms of NO emission in decoupling combustion of coal. *Fuel Process. Technol.* **2006**, *87*, 803−810.

(19) Zhang, J.; Kang, G.; Yang, H.; Liu, Z.; Yu, J.; Gao, S. Co-pyrolysis kinetics and pyrolysis product distribution of various tannery wastes. *J. Fuel Chem. Technol.* **2021**, *49*, 1638−1647.

(20) Liu, J.; Fu, J.; Sun, S.; Zhuo, Z.; Guo, J.; Sun, J.; Wang, Y.; Li, X. Co-combustion of various sources of sludge and its combustion performance. *Acta Sci. Circumstantiae* **2016**, *36*, 940−952.

(21) Kluska, J.; Turzyński, T.; Kardas, D. Experimental tests of co-combustion of pelletized leather tannery wastes and hardwood pellets. *Waste Manage.* **2018**, *79*, 22−29.

(22) Yang, Y.; Ma, H.; Chen, X.; Zhu, C.; Li, X. Effect of incineration temperature on chromium speciation in real chromium-rich tannery sludge under air atmosphere. *Environ. Res.* **2020**, *183*, No. 109159.

(23) Dong, H.; Jiang, X.; Lv, G.; Chi, Y.; Yan, J. Co-combustion of tannery sludge in a commercial circulating fluidized bed boiler. *Waste Manage.* **2015**, *46*, 227−233.

(24) Chen, Y.; Mori, S.; Pan, W. Studying the mechanisms of ignition of coal particles by TG-DTG. *Thermochim. Acta* **1996**, *275*, 149−158.

(25) Shang, X.; Gao, S.; Wang, Y.; Dong, L.; Xu, G.; Guo, J. Comparison of NO_x reduction among different coal combustion methods and the application of decoupling combustion. *J. Fuel Chem. Technol.* **2012**, *4*, 672−679.

(26) Wen, H.; Zhang, G.; Ji, D.; Wan, L.; Zhang, L.; Zhang, Y.; Gao, S. Emission characteristics and control of NO_x from oil sludge char fluidized bed combustion. *J. Fuel Chem. Technol.* **2019**, *47*, 1401−1408.

(27) Kijo-Kleczkowska, A.; Środa, K.; Kosowska, M.; Musial, T.; Wolski, K. Combustion of pelleted sewage sludge with reference to coal and biomass. *Fuel* **2016**, *170*, 141−160.

(28) Niu, X.; Xiao, J. Nitrogen transformation in chemical looping combustion of sewage sludge. *J. Fuel Chem. Technol.* **2017**, *45*, 505−512.

(29) Cai, L.; Shang, X.; Gao, S.; Wang, Y.; Dong, L.; Xu, G. Low-NO_x coal combustion via combining decoupling combustion and gas reburning. *Fuel* **2013**, *112*, 695−703.

(30) Zhai, Y.; Zhu, L.; Chen, H.; Xu, B.; Li, C.; Zeng, G. Experimental investigation on NO_x emission characteristics of a new solid fuel made from sewage sludge mixed with coal in combustion. *Waste Manage. Res.* **2015**, *33*, 157−164.

(31) Zhu, C.; Liu, S.; Liu, H.; Yang, J.; Liu, X.; Xu, G. NO_x emission characteristics of fluidized bed combustion in atmospheres rich in oxygen and water vapor for high-nitrogen fuel. *Fuel* **2015**, *139*, 346−355.

(32) Bai, J.; Yu, C.; Li, L.; Wu, P.; Luo, Z.; Ni, M. Experimental study on the NO and N_2O formation characteristics during biomass combustion. *Energy Fuels* **2013**, *27*, 515−522.

(33) Tomita, A. Suppression of nitrogen oxides emission by carbonaceous reductants. *Fuel Process. Technol.* **2001**, *71*, 53−70.

(34) Kim, D.; Ahn, H.; Yang, W.; Huh, K. Y.; Lee, Y. Experimental analysis of CO/H_2 syngas with NO_x and SO_x reactions in pressurized oxy-fuel combustion. *Energy* **2021**, *219*, No. 119550.

(35) Liao, X.; Shao, J.; Zhang, S.; Li, X.; Yang, H.; Wang, X.; Chen, H. Effects of CO_2 and CO on the reduction of NO over calcined

limestone or char in oxy-fuel fluidised bed combustion. *IET Renewable Power Gener.* **2019**, *13*, 1633−1640.
(36) Lee, B. H.; Song, J. H.; Kim, R. G.; Kim, S. G.; Kim, Y. G.; Chang, Y. J.; Jeon, C. H. Simulation of the influence of the coal volatile matter content on fuel NO emissions in a drop-tube furnace. *Energy Fuels* **2010**, *24*, 4333−4340.
(37) Yin, A.; Deng, W.; Ma, J.; Su, Y. Properties on NO removal over pyrolyzed sludge carbon. *J. Ind. Eng. Chem.* **2018**, *69*, 2655−2663.
(38) Zawadzki, J.; Wisniewski, M. Adsorption and decomposition of NO on carbon and carbon-supported catalysts. *Carbon* **2002**, *40*, 119−124.
(39) Zhang, H.; Jiang, X.; Liu, J.; Shen, J. New insights into the heterogeneous reduction reaction between NO and char-bound nitrogen. *Ind. Eng. Chem. Res.* **2014**, *53*, 6307−6315.
(40) Yang, Y.; Ma, H.; Chen, X.; Zhu, C.; Li, X. Effect of incineration temperature on chromium speciation in real chromium-rich tannery sludge under air atmosphere. *Environ. Res.* **2020**, *183*, No. 109159.
(41) Kanagaraj, J.; Babu, N.; Mandal, A. Recovery and reuse of chromium from chrome tanning waste water aiming towards zero discharge of pollution. *J. Cleaner Prod.* **2008**, *16*, 1807−1813.

https://doi.org/10.1021/acsomega.1c05640
ACS Omega 2022, 7, 4110−4120